Commun. Theor. Phys. (Beijing, China) **53** (2010) pp. 560–564

Vol. 53, No. 3, March 15, 2010

Noise Shielding Using Acoustic Metamaterials*

LIU Bin (刘斌) and HUANG Ji-Ping (黄吉平)†

Department of Physics and Surface Physics Laboratory (National Key Laboratory), Fudan University, Shanghai 200433, China

(Received March 30, 2009; revised manuscript received June 17, 2009)

Abstract *We exploit theoretically a class of rectangular cylindrical devices for noise shielding by using acoustic metamaterials. The function of noise shielding is justified by both the far-field and near-field full-wave simulations based on the finite element method. The enlargement of equivalent acoustic scattering cross sections is revealed to be the physical mechanism for this function. This work makes it possible to design a window with both noise shielding and air flow.*

PACS numbers: 43.20.+g, 43.35.+d, 43.40.+s
Key words: general linear acoustics, ultrasonics, quantum acoustics, physical effects of sound, structural acoustics and vibration

1 Introduction

Recently, a new device, "electromagnetic (EM) superscatterer", was proposed by Ma and his coworkers using a pair of EM complementary media.[1−4] The EM scattering cross section of such an EM superscatterer appears to be bigger than its physical size in an EM wave detection, so it can be used to enhance the EM wave scattering cross section of an object.[1] Both circular cylindrical[1] and rectangular cylindrical[2] EM superscatterers were designed in two dimensions (2D), and they were justified by finite-element full-wave numerical simulations. Some interesting applications of 2D EM superscatterers such as concealing entrances were also demonstrated.[2]

A trend in metamaterial-based research is to generalize the EM cases to other fields, such as acoustics[5−8] and thermodynamics,[9] in order to achieve new applications. With the successful precedent of EM superscatterers,[1−3] a natural, but potentially important, question would be the feasibility of acoustic superscatterers. If successful, they may give birth to important applications like noise shielding of our interest. In the mean time, it may also enrich the realm of the study of acoustic waves.[10−11]

This paper is organized as follows. In Sec. 2, we present the theoretical formalism. In Sec. 3, the results are given according to the full-wave simulations based on the finite element method. This paper ends with a discussion and conclusion in Sec. 4.

2 Theory

The theoretical feasibility of 2D acoustic superscatterers, if any, depends on the invariance property of the acoustic equation in time harmonic form

$$\vec{\nabla}\cdot\Big[\frac{1}{\rho(x,y)}\vec{\nabla}p(x,y)\Big]+\frac{\omega^2}{\lambda(x,y)}p(x,y)=0\,, \qquad (1)$$

where

$$\vec{\nabla}=\frac{\partial}{\partial x}\vec{i}+\frac{\partial}{\partial y}\vec{j}\,,$$

Here $p(x,y)$ and ω are the pressure field at position (x,y) and angular frequency of an incident acoustic wave, respectively. Then the coordinate transformation method can be used to obtain the anisotropic mass density tensor $\rho(x,y)$ and the bulk modulus $\lambda(x,y)$ to design an acoustic superscatterer. The specific deduction can draw inspiration from the equivalence between acoustics and electromagnetics in 2D. Cummer and Schurig[6] demonstrated that in a 2D geometry, the acoustic equations in a fluid are identical in form to the single polarization Maxwell equations via a variable exchange that also preserves boundary conditions. Since the function of EM superscatterers in an incident transverse-electric (TE) polarized EM field with harmonic time dependence $\exp(-i\omega t)$ was thoroughly verified in both the analytical and numerical ways, we may expect the same function of acoustic superscatterers in the presence of an incident pressure acoustic field with harmonic time dependence.

To demonstrate the similarity and difference between 2D EM superscatterers and acoustic superscatterers, we use a geometric model, which is similar to that adopted in Ref. [2], see Fig. 1. Initially, we consider a rectangular cylinder with dimensions $\{2a_3, 2b_3\}$. It has a sound-soft boundary surface, which corresponds to the perfect electrical conductor boundary condition in the case of 2D EM superscatterers. The sound-soft boundary is selected to demonstrate the function of acoustic superscatterers since experimentally a fluid system is the most practical way to realize acoustic metamaterials,[12−13] and in numerical simulations this boundary condition is an appropriate approximation for a liquid-gas interface. The essential step of the design of an acoustic superscatterer

*Support by the National Natural Science Foundation of China under Grant Nos. 10604014 and 10874025, and by Chinese National Key Basic Research Special Fund under Grant No. 2006CB921706
†Corresponding author, E-mail: jphuang@fudan.edu.cn

is the compression of the rectangular cylinder $\{2a_3, 2b_3\}$ into a smaller rectangular cylinder $\{2a_1, 2b_1\}$. We denote the surfaces of these rectangular cylinders as Γ_3 and Γ_1 , respectively. It should be stressed that after the compression, the sound-soft boundary condition Γ_3 is mapped to the surface Γ_1. Then we fill the gap between Γ_1 and Γ_3 with a pair of complementary media: between Γ_2 and Γ_3 is the same media as those beyond Γ_3; between Γ_1 and Γ_2 is the acoustic metamaterials with anisotropic mass density tensors. Now Γ_2 serves as the outer rectangular surface of the acoustic-metamaterial shell. As the name "superscatterer" indicates, it is expected that the device $\{2a_2, 2b_2\}$ with physical outer surface Γ_2 scatters the same acoustic fields as the uncompressed rectangular cylinder $\{2a_3, 2b_3\}$ once the acoustic-metamaterial shell satisfies appropriate conditions yet to be determined.

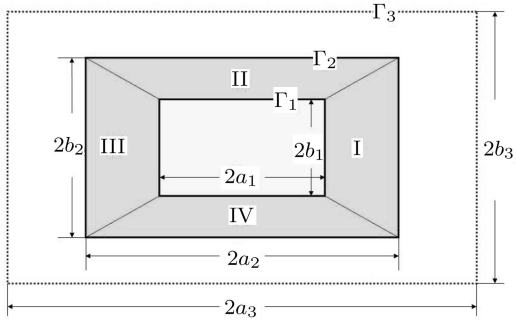

Fig. 1 Schematic graph showing the design of a rectangular cylindrical acoustic superscatterer with sizes $\{2a_2, 2b_2\}$ by filling acoustic metamaterials into the shell between the surfaces Γ_1 and Γ_2. The dashed line denotes a virtual rectangular cylinder with $\{2a_3, 2b_3\}$ and surface Γ_3 whose scattering cross section is the same as that of the superscatterer with smaller sizes $\{2a_2, 2b_2\}$. The relevant parameters, a_1, a_2, a_3, b_1, b_2, and b_3, are indicated in the graph. For the simulations in Figs. 2–3, arbitrary materials can be inserted within Γ_1.

The parameters of the acoustic-metamaterial shell can be obtained according to the coordinate transformation method. Here we choose a simple continuous map between the pair of complementary media: The region between Γ_2 and Γ_3 is mapped to the region between Γ_1 and Γ_2. Especially, the surface Γ_3 is mapped to Γ_1, but the surface Γ_2 is mapped to itself. As shown in Fig. 1, the shell is divided into four regions (I, II, III, and IV), and the coordinate transformation equations for region I read

$$x' = -\frac{a_2 - a_1}{a_3 - a_2}x + \frac{a_3 - a_1}{a_3 - a_2}a_2\,, \tag{2}$$

$$y' = -\frac{a_2 - a_1}{a_3 - a_2}y + a_2\frac{a_3 - a_1}{a_3 - a_2}\frac{y}{x}\,, \tag{3}$$

$$z' = z\,. \tag{4}$$

But the difference in deduction of material parameters begins as we proceed. Now we have the Jacobian transformation matrix between the original coordinates (x, y, z) and the transformed coordinates (x', y', z'): $\Lambda_i^{i'} = \partial x^{i'}/\partial x^i$. Here the subscript $i = x, y$, and z, and $i' = x', y'$, and z'. Similar notations hold for the following subscripts j, j', k, k', l, and l'. Cummer and Schurig[6] gave the general transformation equations for the mass density tensor $\rho_{i'j'}$ and the bulk modulus λ' under the 2D coordinate transformation

$$\rho_{i'j'} = \det(\Lambda)^{-1}(\epsilon_{i'k'z}\Lambda_k^{k'}\epsilon_{kiz})(\epsilon_{j'l'z}\Lambda_l^{l'}\epsilon_{ljz})\rho_{ij}\,, \tag{5}$$

$$\lambda' = \det(\Lambda)(\Lambda_z^{z'})^{-2}\lambda\,. \tag{6}$$

Since we consider the case that the mass density and the bulk modulus of the materials outside the surface Γ_3 is uniform, namely, $\rho_{ij} = \rho_0\delta_j^i$, Eq. (5) can be re-expressed as

$$\rho_{x'x'} = \det(\Lambda)^{-1}((\Lambda_x^{y'})^2 + (\Lambda_y^{y'})^2)\rho_0\,, \tag{7}$$

$$\rho_{x'y'} = \rho_{y'x'} = -\det(\Lambda)^{-1}(\Lambda_x^{x'}\Lambda_x^{y'} + \Lambda_y^{x'}\Lambda_y^{y'})\rho_0\,, \tag{8}$$

$$\rho_{y'y'} = \det(\Lambda)^{-1}((\Lambda_x^{x'})^2 + (\Lambda_y^{x'})^2)\rho_0\,. \tag{9}$$

For region I, using the coordinate transformation Eqs. (2)–(4), we obtain the mass density tensor ρ and the bulk modulus λ as follows

$$\rho_{x'x'} = -\frac{(a_3 - a_2)^2x'^4 + a_2^2(a_3 - a_1)^2y'^2}{(a_3 - a_2)x'^3\Delta}\rho_0\,, \tag{10}$$

$$\rho_{x'y'} = \rho_{y'x'} = \frac{a_2(a_3 - a_1)y'}{(a_3 - a_2)x'^2}\rho_0\,, \tag{11}$$

$$\rho_{y'y'} = -\frac{\Delta}{(a_3 - a_2)x'}\rho_0\,, \tag{12}$$

$$\lambda' = -\frac{(a_2 - a_1)^2x'}{(a_3 - a_2)\Delta}\lambda\,, \tag{13}$$

where $\Delta = (a_3 - a_1)a_2 - (a_3 - a_2)x'$. Similarly, we can obtain the material parameters in regions II, III, and IV, respectively. It should be noted that the obtained material parameters are not continuous at the interfaces between the four regions, which, however, does not harm the role of the proposed acoustic superscatterers, as to be shown in Figs. 2–3. In principle, acoustic metamaterials with the properties determined by Eqs. (10)–(13) can be realized by using local resonances.[12,14−16]

3 Results

For numerical simulations, we resort to the commercial finite element simulation package COMSOL Multiphysics 3.5. For the simulations, we choose the geometric parameters $\{a_1, a_2, a_3\}$ and $\{b_1, b_2, b_3\}$ as $\{0.03\,\text{m}, 0.06\,\text{m}, 0.12\,\text{m}\}$ and $\{0.015\,\text{m}, 0.03\,\text{m}, 0.06\,\text{m}\}$, respectively.

Figure 2 displays the case of an incident acoustic plane wave with unit amplitude and frequency 10 000 Hz, to mimic far-field cases. The environment outside the superscatterer with dimensions $\{2a_2, 2b_2\}$ is filled with air, and the plane wave under our consideration has a wavelength of 0.034 m or so. [It should be mentioned that any (equivalently) homogeneous acoustic media, such as air, (pure)

fluids, or suspensions, can be selected as the environmental media. Here we choose air for simplicity]. In Fig. 2, the uppermost and lowermost plates are perfect matched layer (PML) regions, absorbing the reflected waves to guarantee the accuracy of the simulations. Figure 2(a) displays the pressure field distribution when the plane wave is blocked and reflected by an intact uniform wall with a sound-soft boundary surface. As expected, a standing acoustic wave forms. In Fig. 2(b), we remove a central part of the wall to make a rectangular path with dimensions $\{2a_3, 2b_3\}$, allowing the flow of a part of the incident plane wave. In Fig. 2(c), a uniform rectangular cylindrical object with dimensions $\{2a_2, 2b_2\}$ and a sound-soft boundary surface is placed at the center of the path, as indicated in the figure. The intensity of acoustic waves traveling around the object is reduced when compared with Fig. 2(b). Figure 2(d) demonstrates the performance of the acoustic superscatterer with dimensions $\{2a_2, 2b_2\}$. As expected, the superscatterer has the same function of scattering acoustic waves as the uniform rectangular cylinder with $\{2a_3, 2b_3\}$ [see Fig. 2(a)] since (almost) no wave penetrates through the path. Since the bounds of the amplitude of pressure fields in Fig. 2 is set from -2 to 2 for clarity, the regions where the value of amplitude exceeds the bounds appear to be white. The comparison between Figs. 2(a) and 2(d) confirm convincingly the function of noise shielding by using acoustic metamaterials appropriately, while allowing the flow of air.

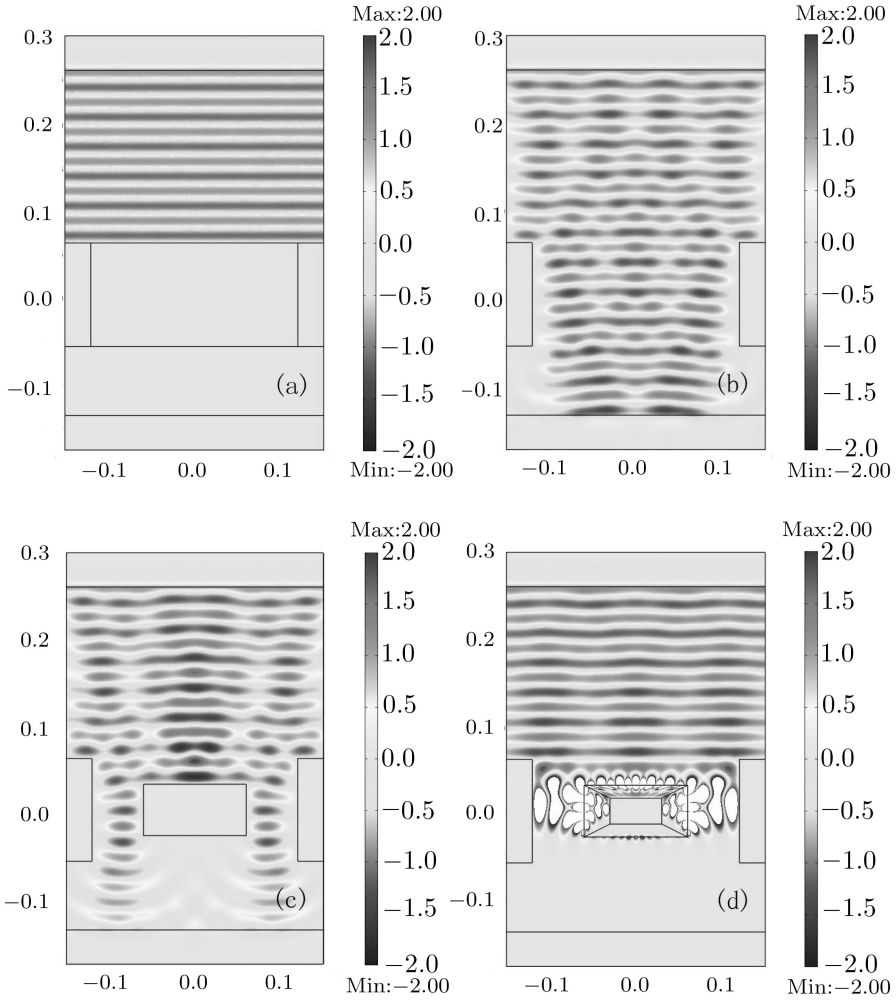

Fig. 2 Snapshot of the distribution of the pressure field induced by an incident plane wave. (a) The pressure field distribution caused by a uniform rectangular cylinder with dimensions $\{2a_3, 2b_3\}$ and a sound-soft boundary surface; (b) The pressure field distribution with a path unblocked by a rectangular cylindrical area with $\{2a_3, 2b_3\}$; (c) The pressure field distribution with a path blocked by a uniform rectangular cylinder with $\{2a_2, 2b_2\}$ and a sound-soft boundary surface; (d) The pressure field distribution for an acoustic superscatterer with $\{2a_2, 2b_2\}$. In Fig. 2(d), the acoustic wave is totally reflected so that the pressure field on the other side of the path seems to disappear (or concretely, becomes weak enough to be neglected). Alternatively, from the noise-shielding point of view, (d) plays the same role as (a). In Figs. 2(a)–2(d), the upper-most and lower-most plates are PML regions, which absorb the reflected waves.

Similar behaviors appear in Fig. 3 which displays an incident cylindrical acoustic wave in order to model a near-field

case. Thus, we may claim that this work is of potential value for designing a window with both noise shielding and air flow.

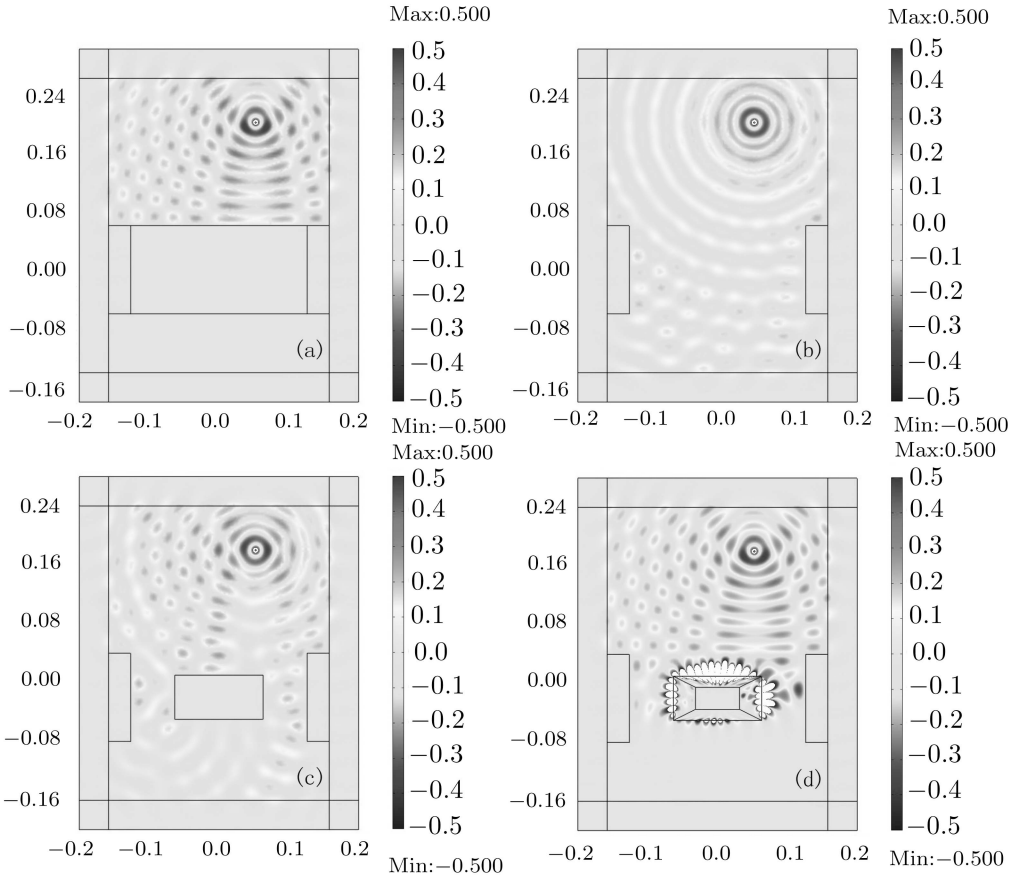

Fig. 3 The same as Fig. 2, but for an incident cylindrical wave with its source located at (0.05 m, 0.2 m). PML regions are placed around the central simulation area.

4 Discussion and Conclusion

In this work we have designed an acoustic device for noise shielding by means of a rectangular superscatterer based on acoustic metamaterials. This superscatterer has been designed with the help of a coordinate transformation that maintains the acoustic wave equation invariant. A difficult item is possibly to discuss the viability of building the metamaterials required, which is the real difference between electromagnetic and acoustic phenomena. For our design, the acoustic properties of the rectangular superscatterer have to be negative, which seems to be doable due to the recent experimental breakthrough in the field.[16] It is worth noting that, although metamaterials with these properties are, in principle, possible, they are not broadband and noise shielding devices, normally, require broadband functionality. In this sense, being beyond the basic principle presented in this work, much more work is subjected to be further studied along this direction.

Throughout this work, we have not taken into account the absorption of acoustic waves. In fact, if we consider the existence of absorption, the function of the proposed acoustic superscatterers and hence the desired noise shielding holds as well.

In conclusion, following Ma and his coauthors' "EM superscatterers", we have designed theoretically a class of acoustic superscatterers using acoustic metamaterials, with the shape of a rectangular cylinder. Their function of noise shielding has been fully demonstrated by the full-wave simulations. It has been revealed that the enlargement of equivalent scattering cross sections serves as the underlying physical mechanism. This work makes it possible to design windows with both noise shielding and air flow.

Acknowledgments

We thank Professor S.A. Cummer for his helpful advice.

References

[1] T. Yang, H. Chen, X. Luo, and H. Ma, Opt. Express **16** (2008) 18545.

[2] X. Luo, T. Yang, Y. Gu, and H. Ma, arXiv:0809.1823v1.

[3] H. Chen, X. Zhang, X. Luo, H. Ma, and C.T. Chan, New J. Phys. **10** (2008) 113016.

[4] http://www.nature.com/news/2008/080919/full/news.2008.1113.html

[5] H. Chen and C.T. Chan, Appl. Phys. Lett. **91** (2007) 183518.

[6] S.A. Cummer and D. Schurig, New J. Phys. **9** (2007) 45.

[7] S.A. Cummer, B.I. Popa, D. Schurig, D.R. Smith, J. Pendry, M. Rahm, and A. Starr, Phys. Rev. Lett. **100** (2008) 024301.

[8] B. Liu and J.P. Huang, Eur. Phys. J. Appl. Phys. **48** (2009) 20501.

[9] C.Z. Fan, Y. Gao, and J.P. Huang, Appl. Phys. Lett. **92** (2008) 251907.

[10] M.M. Lin and W.S. Duan, Commun. Theor. Phys. **47** (2007) 339.

[11] S.J. Yang, H. Zhao, and Y. Yu, Commun. Theor. Phys. **44** (2005) 1095.

[12] J. Li and C.T. Chan, Phys. Rev. E **70** (2004) 055602.

[13] N. Fang, D. Xi, J. Xu, M. Ambati, W. Srituravanich, C. Sun, and X. Zhang, Nat. Mater. **5** (2006) 452.

[14] Z. Liu, X. Zhang, Y. Mao, Y.Y. Zhu, Z. Yang, C.T. Chan, and P. Sheng, Science **289** (2000) 1734.

[15] J. Mei, Z. Liu, W. Wen, and P. Sheng, Phys. Rev. Lett. **96** (2006) 024301.

[16] Z. Yang, J. Mei, M. Yang, N.H. Chan, and P. Sheng, Phys. Rev. Lett. **101** (2008) 204301.